Hierarchical ZSM-5 zeolites synthesized by silanization of protozeolitic units: mediating the mesoporosity contribution by changing the organosilane type

D. P. Serrano[1,2]*, T. J. Pinnavaia[3], J. Aguado[4], J. M. Escola[4], A. Peral[1], L. Villalba[1]

[1]Department of Chemical and Energy Technology, ESCET
Rey Juan Carlos University, Móstoles, 28933, Spain

[2]Madrid Institute for Advanced Studies on Energy
IMDEA Energy, Móstoles, 28933, Spain

[3]Department of Chemistry, Michigan State University
East Lansing, MI 48823, USA

[4]Department of Chemical and Environmental Technology, ESCET
Rey Juan Carlos University, Móstoles, 28933, Spain

Published on:

Catalysis Today, 227 (2014) 15-25. doi: 10.1016/j.cattod.2013.10.052

---

* to whom correspondence should be addressed
e-mail: david.serrano@urjc.es

Tel: +34 91 488 74 50, Fax: +34 91 488 70 68

Abstract

Hierarchical ZSM-5 zeolites were prepared by crystallization of silanized protozeolitic units employing silylated polypropylene oxide diamine polymers as organosilanes. The influence of the (Si_{pol}/ Si_{gel}) molar ratio was investigated within 0 - 0.15 range. High synthesis yields (~90%) of well-crystallized hierarchical zeolites exhibiting a high proportion of secondary porosity (additional to the zeolitic micropores) was reached for (Si_{pol}/Si_{gel}) molar ratios lower than 0.08. The usage of the silylated polymer resulted in hierarchical ZSM-5 with larger mesopores (4-20 nm) in higher share than the hierarchical ZSM-5 prepared with a smaller organosilane (phenyl-aminopropyl-trimethoxysilane, PHAPTMS). However, it also contained meaningfully lower amount of acid sites and with less acid strength. The best catalytic performance in the cracking of low density polyethylene (LDPE) was showed by the material prepared from a (Si_{pol}/Si_{gel}) ratio of 0.03. Noteworthy, in addition to the gasoline range fraction (C_6-C_{12}), light C_1-C_5 olefins are the main reaction products, which are interesting feedstock for the petrochemical industry. Its catalytic performance is similar to the hierarchical ZSM-5 prepared using the smaller organosilane (PHAPTMS), which is indicative that the enhanced accessibility to the acid sites due to the presence of larger mesopores (4 – 20 nm) makes up for the lower amount and strength of its acid sites. Thereby, it is possible to enhance the mesoporosity by using bulkier organosilane (silylated polymers) but at the expense of losing acid properties.

Keywords: hierarchical porosity, ZSM-5, silanization, silylated polymer, PHAPTMS

1. Introduction

Hierarchical zeolites exhibiting at least two levels of pore sizes have attracted great interest in the last years [1-4]. These materials combine the typical zeolitic micropores with the occurrence of additional secondary porosity (e.g. supermicropores, mesopores, macropores), which is an advantage when these catalysts are applied in reactions involving bulky compounds. Improved catalytic performance is exhibited by hierarchical zeolites if compared with traditional ones due to several factors [1]: a reduction of the steric limitations for converting large molecules, an increase in the rate of intracrystalline diffusion [5-7], an enhanced selectivity towards desired products in some reactions [8,9] and a decrease in deactivation phenomena by coke deposition [10,11]. In view of these advantages a wide variety of methods aimed at creating additional or secondary porosity into zeolitic structures have been developed in the last years [1, 11-28]: post-synthesis treatments, such as dealumination [12] and desilication [13-15], based on the removal of framework atoms, dual templating with surfactants [16,17], geminisurfactants [18] or cationic polymers [19], hard-templating methods employing carbonaceous [20,21] or polymeric templates [22,23], and silanization based methods such as the crystallization using amphiphilic organosilanes [24] or silylated polymers [25,26]. In the later case, mesoporous ZSM-5 zeolites with intracrystal mesopores were obtained by adding to the initial synthesis gel a silylated polymer, formed by the reaction of (3-glycidoxypropyl)trimethoxysilane and polyethyleneimine or polypropylene oxide diamine polymers. Catalysts having average intracrystal pore sizes in the range from 2 nm to 5 nm were obtained by adjusting the nature and molecular weight of the polymer, boosting not only the reactivity, but also the product selectivity towards propylene and butylenes in gas-oil cracking reactions in comparison to conventional ZSM-5 [26].

Another silanization-based method is the crystallization of silanized protozeolitic nanounits [27,28]. This synthesis strategy named as protozeolitic units silanization, comprises several steps. Firstly, the initial clear solution is precrystallized at low temperature (from room

temperature to 90º C) to promote the formation of protozeolitic nanounits. Secondly, organosilanes of the type $RSi(OR)_3$ are added over protozeolitic nanounits previously formed, to promote the functionalization of their external surface by reaction with the organosilane. Finally, crystallization is performed to complete the zeolitization of silanized protozeolitic nanounits. The presence of the organosilane anchored on the external surface of the zeolitic nanounits prevents the aggregation of the nanoparticles into larger crystals during this final hydrothermal treatment at high temperature. The product finally obtained applying this strategy consist of aggregates of ultra-small zeolite nanocrystals (5-20 nm) exhibiting intracrystal mesopores. This strategy has proven to be a versatile method applicable to the syntheses of a variety of hierarchical zeolites: ZSM-5 [27], ZSM-11 [29], A [30], Beta [27,31], Mordenite [32], and TS-1 [33].

Interestingly, the properties of zeolites synthesized by crystallization of silanized protozeolitic nanounits can be tailored modifying the synthesis conditions. In the case of ZSM-5, the time and temperature of the precrystallization stage, and the nature and concentration of organosilane, are essential factors which determine its textural and acid properties [28, 34-37]. Moreover adding alcohols mixed with the organosilane in the silanization stage may also improve the textural properties and catalytic performance of ZSM-5 in the cracking of polyolefins [38]. In respect of the precrystallization stage, if this step is omitted and the organosilane is mixed directly with the initial synthesis solution (containing the silica and alumina sources and the organic structure directing agent), no crystalline material is obtained [28]. It also was found that decreasing the temperature of the precrystallization step, hierarchical ZSM-5 zeolites with improved textural properties were achieved. Furthermore, the molar ratio organosilane/silica source (Si_{silane}/Si_{gel}) in the synthesis gel during the silanization step is also a controlling factor and the proper concentration depends on the nature of the organosilane added. In this regards, it was found that adding phenylaminopropyltrimethoxysilane (PHAPTMS) an optimum in the textural properties of the final product was attained employing a 0.12 Si_{silane}/Si_{gel} molar ratio [28].

However, if N-(vinylbenzyl)-2-aminoethyl-3-aminopropyl-trimethoxysilane is used the optimum organosilane content is found in the range 0.05-0.07 [35].

The nature of the organosilane plays also a vital role on the textural and catalytic properties of the hierarchical ZSM-5 prepared by seed silanization [34, 36-37]. Until the present date, among the different organosilanes tested by our group, mainly small $RSi(OR)_3$ silanes, PHAPTMS has resulted on the best silanization agent due to its effective interaction with the external surface of the protozeolitic nanounits [36]. However due to the huge number of organosilanes available, differing in size and nature, a variety of alternatives for the synthesis of hierarchical zeolites by crystallization of protozeolitic nanounits are opened [1].

In this work, we firstly show the possibility to broaden the seed silanization strategy by using bulkier silylated polymers as organosilanes. Thereby, the effect of the (Si_{pol}/Si_{gel}) molar ratio added during the silanization stage on the textural properties of the obtained hierarchical ZSM-5 was determined, in order to set up the suitable conditions for attaining hierarchical ZSM-5 of the highest quality. This hierarchical zeolite was subsequently tested in the cracking of low density polyethylene (LDPE) and their results compared to those attained using a hierarchical ZSM-5 prepared employing phenyl-aminopropyl-trimethoxysilane (PHAPTMS) as organosilane. Henceforth, the obtained results are reported.

2. Experimental

a) Synthesis of hierarchical ZSM-5 samples

Hierarchical ZSM-5 zeolite samples were prepared by crystallization of silanized protozeolitic nanounits modifying a procedure published elsewhere [27]. The precursor ZSM-5 zeolite solutions were prepared with the following molar composition: 1 Al_2O_3 : 60 SiO_2 : 11

TPAOH : 1500 H_2O. Tetraethoxysilane (TEOS, 98%; Aldrich) and aluminum isopropoxide (AIP; Aldrich), as silica and alumina source, respectively, tetrapropyl-ammonium hydroxide (TPAOH, 40%; Alfa) as structure directing agent (SDA), and distilled water, were used as starting materials. The precursor solutions were aged at ambient temperature for 40 h and then the clear solutions obtained were precrystallized under reflux, with stirring (100 rpm), at 90 ºC for 20 h. Then, the protozeolitic units were functionalized with a silylated polymer [2] at 90ºC, the $Si_{polymer}/Si_{precursor\ solution}$ molar ratio (Si_{pol}/Si_{gel}) ranging from 0.0 to 0.15. The silylated polymer was formed by reaction of (3-glycidoxypropyl)trimethoxysilane (Aldrich) with polypropylene oxide diamine (Jeffamine D-400, Huntsman) at a Si/NH ratio of 0.1. After the silanization stage, crystallization was carried out in Teflon®-lined stainless-steel autoclaves under static conditions and under autogeneous pressure for 8 days at 150ºC. Finally, the solid products obtained were separated by centrifugation, washed several times with distilled water, dried overnight at 110 ºC and calcined in air at 600 ºC for 5 h.

Additionally, a hierarchical ZSM-5 zeolite was synthesized following also the crystallization of silanized protozeolitic nanounits but substituting the silylated polymer for phenyl-aminopropyl-trimethoxysilane (PHAPTMS; Aldrich) as organosilane. In this case, the silanization reaction was performed employing a $Si_{PHAPTMS}/Si_{precursor\ solution}$ molar ratio ($Si_{PHAPTMS}/Si_{gel}$) equal to 0.05. This hierarchical reference sample was denoted as ZSM-5 (PHAPTMS).

b) Characterization of hierarchical ZSM-5 samples

The samples were characterized by means of conventional techniques. Fourier transform infrared (FTIR) spectra were recorded in a Varian Excalibur Series 3100 spectrophotometer with a resolution of 4 cm^{-1} using the KBr pellet technique. Powder X-ray diffraction (XRD) patterns were measured using a Philips X´PERT MPD diffractometer (Cu K_α radiation) with step size and

counting time of 0.02º and 10 s, respectively. Nitrogen adsorption-desorption isotherms at 77 K were obtained in a Micromeritics ASAP 2010 instrument, whereas argon adsorption-desorption isotherms at 87 K were acquired using a Quantachrome Autosorb 1 MP automated gas sorption system. In both cases, the analyses were carried out after outgassing the samples at 300 ºC under vacuum for 16 h. BET surface analyses have been performed using the relative pressure range of 0.05 to 0.16. The Si/Al atomic ratios of the catalysts were determined by inductively coupled plasma spectroscopy (ICP) with a VARIAN VISTA AX apparatus, while elemental chemical analyses for C, N, H were carried out using a Vario EL III instrument. Thermogravimetric (TGA) analyses were performed using a SDT 2960 instrument, and transmission electron microscopy (TEM) images were obtained with a JEOL 2000 electron microscope operating at 200 kV. Finally, solid-state ^{27}Al NMR experiments were conducted at room temperature on a Varian Infinity Plus 400 spectrometer operating at frequencies of 104.16 MHz. ^{27}Al chemical shifts were referenced to $Al(H_2O)_6^{3+}$ as external standard and (MAS) NMR spectra were obtained using spinning rates of 12 kHz. . Temperature-programmed desorption of ammonia (NH_3 TPD) measurements were carried out in a Micromeritics AutoChem 2910 system using He as carrier gas. Previously, the samples were outgassed under a helium flow (50 Nml min^{-1}) with a heating rate of 15ºC min^{-1} up to 560 ºC and kept at this temperature for 30 min. After cooling to 180 ºC, an ammonia flow of 35 Nml min^{-1} was passed through the sample for 30 min. Once the physisorbed ammonia was removed by flowing helium at 180 ºC for 90 min, the chemisorbed ammonia was determined by increasing the temperature with a heating rate of 15 ºC min^{-1} up to 550 ºC, keeping constant this temperature for 30 min. The ammonia concentration in the effluent helium stream was monitored with a thermal conductivity detector (TCD). The Brönsted acid sites of selected samples were also measured by cationic-exchange using a NaCl as exchanging agent. In a typical experiment, 0.05 g of zeolite was added to 20 g of NaCl (aq, 1M), the aqueous

solution being maintained under stirring at 60 ºC for 6 hours. Released protons were then potentiometrically titrated by addition of 0.01 M NaOH aqueous solution.

c) Catalytic cracking of LDPE

Catalytic properties of the hierarchical ZSM-5 samples were tested for the cracking of low density polyethylene (LDPE, Repsol) following a procedure published elsewhere [37]. The reactions were carried out in a stainless steel batch reactor provided with a helicoidal stirrer swept by a continuous nitrogen flow (35 $mL \cdot min^{-1}$) to ensure that the LDPE conversion takes place under inert conditions and to favor the removal of the volatile products. In a typical experiment, 10 g of LDPE were introduced into the reactor together with 0.1 g of the catalyst (LDPE/catalyst mass ratio of 100, P/C=100). The reactor was heated up to the reaction temperature (320 or 340 ºC) in 30 min, and thereafter it was kept constant for the reaction time (2h). Gaseous and liquid products leaving the reactor were separated in a condenser at 0 ºC and collected. A Varian 3800 gas chromatograph, using a 100 m length x 0.25 mm i.d. Chrompack capillary column, was used to analyze both gaseous and liquid fractions.

3. Results and Discussion

Crystallization of silanized protozeolitic nanounits has demonstrated to be a versatile method applicable to the synthesis of a variety of hierarchical zeolites [29-33]. Small $RSi(OR)_3$ silanes have been usually employed for the synthesis of hierarchical ZSM-5 zeolites. However, the large number of organosilanes available, differing in size, chemical composition and nature, opens up a variety of alternatives for the synthesis of hierarchical zeolites [1]. In this work, we have explored the possibility to widen the protozeolitic units silanization strategy by using a

bulkier silylated polymer as organosilane. Accordingly, the influence of the $Si_{polymer}/Si_{gel}$ molar ratio added to the synthesis medium during the silanization stage was studied and the main physicochemical properties of the obtained materials was determined.

XRD patterns of the calcined samples prepared from the crystallization of silanized protozeolitic nanounits employing the silylated polypropylene oxide diamine polymer as the organosilane are displayed in Figure 1.A. The materials prepared employing a Si_{pol}/Si_{gel} molar ratio ranging from 0.0 to 0.10 are clearly crystalline and show the typical pattern of the MFI zeolitic structure. Strong and sharp diffraction peaks are observed in these samples, although with lower intensity than the observed ones in the XRD patterns of the zeolite prepared without silylated polymer. This fact might be ascribed to the smaller crystalline domains present in these materials in regard to the reference sample. This effect is much more marked in the sample synthesized with a Si_{pol}/Si_{gel} ratio = 0.12, wherein the lowest intensity peaks were observed. On the other hand, the sample synthesized employing the highest Si_{pol}/Si_{gel} ratio in the silanization stage (0.15) shows the diffraction pattern characteristic of an amorphous material.

FTIR spectra depicted in Figure 1.B confirm these XRD results. The band at 1220 cm^{-1} has been assigned to the T-O-T asymmetric stretching mode, and is characteristic of well crystallized zeolites, while the band at 550 cm^{-1} has been assigned to the asymmetric stretching mode of the five-membered rings of ZSM-5 zeolite, being absent in amorphous solids [39,40]. Both bands are clearly observed in the materials prepared with a Si_{pol}/Si_{gel} ratio ≤ 0.10, but are hardly expressed or absent in the samples synthesized with a Si_{pol}/Si_{gel} ratio of 0.12 and 0.15, respectively. Moreover, the intensity of both bands decreases when the proportion of silylated polymer employed in the synthesis increases, indicating that the presence of a higher proportion of this bulky organosilane in the medium hinders the crystallization of ZSM-5 zeolites. Coudurier y col. [40] postulated the ratios of optical densities (ODR) of the 550 cm^{-1} and 450 cm^{-1} bands as a good probe to characterize the presence of a zeolite framework, reporting that for a well

crystallized ZSM-5 zeolite the ratio is close to 0.7. ODR of the materials prepared employing different Si_{pol}/Si_{gel} molar ratio are given in Table 1. This value diminishes as the Si_{pol}/Si_{gel} ratio employed in the synthesis increases, being below 0.7 when this ratio is higher than 0.10.

TEM micrographs of the materials prepared with different Si_{pol}/Si_{gel} molar ratio are shown in Figure 2. No presence of a significant amount of amorphous phase is detected in the samples prepared with a Si_{pol}/Si_{gel} ratio ≤ 0.08, while a coexistence of well formed crystalline domains and non-crystalline material is observed in rest of the samples. An increase in the presence of the amorphous phase is observed as the Si_{pol}/Si_{gel} molar ratio employed in the silanization stage is increased. This fact bears out the observations derived from XRD and FTIR data. Well formed nanocrystals with sizes ranging from 40 to 100 nm are present in the reference sample (figure 2a), synthesized in the absence of silylated polymer. When a Si_{pol}/Si_{gel} ratio = 0.03 is employed in the silanization stage aggregates with sponge-like morphology are obtained (figure 2b). The aggregates present a size that ranges between 200 and 800 nm, and are made up of well-formed and very small crystallites of about 10 nm (figure 2c). The sample organofunctionalized employing a Si_{pol}/Si_{gel} ratio = 0.05 (figure 2d) shows a morphology similar to that of the material prepared using a Si_{pol}/Si_{gel} ratio = 0.03. Small particles partially aggregated constituting sponge-like structures with sizes up to 800 nm are observed in this sample. However, a higher degree of aggregation of the small units is evident in this sample in comparison with the material prepared with a Si_{pol}/Si_{gel} ratio = 0.03 and individual crystallites are hardly detected. Moreover, clearly visible intercrystalline voids can be appreciated in both samples. Detailed analysis of a variety of TEM micrographs reveals the presence of voids as small as 3 nm, and as larger as 170 nm, in the sample prepared employing a Si_{pol}/Si_{gel} ratio = 0.03. Smaller intercrystalline voids, with sizes even lower than 3 nm, are present in a higher proportion in the material synthesized using a Si_{pol}/Si_{gel} ratio = 0.05. Aggregates with sizes from 200 to 800 nm built by highly packed crystalline particles constitutes the main phase of the sample prepared employing a Si_{pol}/Si_{gel} ratio = 0.08

(figure 2e), although a small proportion of non-crystalline phase is detected mainly surrounding the crystalline aggregates. Similar aggregates are observed in the samples prepared by using Si_{pol}/Si_{gel} ratios = 0.10 ((figures 2f and 2g)) and 0.12 (figure 2h), but in these cases the aggregates are embedded in micrometer-size amorphous particles. In both materials, the amorphous phase is in the majority, although its proportion is higher in the sample prepared with a Si_{pol}/Si_{gel} ratio = 0.12.

Figure 3 illustrates the ^{27}Al NMR spectra of some selected samples prepared with a different Si_{pol}/Si_{gel} ratio. The calcined sample prepared with a Si_{pol}/Si_{gel} ratio = 0.03 presents mostly tetrahedral aluminium (Al^{IV} = 89%) incorporated into the framework, the amount of octahedral aluminium being quite low (Al^{VI} = 11%). Moreover, only a very slight increase in the share of octahedral aluminium is detected when the Si_{pol}/Si_{gel} molar ratio is increased. Thus, the octahedral aluminium content is increased from 12% in the sample prepared from a Si_{pol}/Si_{gel} ratio = 0.05, to only 13% when a Si_{pol}/Si_{gel} ratio = 0.12 was added in the silanization stage. However, the full width at half maximum (FWHM) varies from values close to 7.5 ppm in the samples prepared from a low Si_{pol}/Si_{gel} ratio (0.03 and 0.05), to more than 11 ppm in the material prepared from a Si_{pol}/Si_{gel} ratio = 0.12, confirming its mostly amorphous nature of the latter products. Thereby, the samples prepared at a low proportion of silylated polymer possess well ordered aluminium environments. Note that nanocrystalline ZSM-5 samples, very similar in size and composition to the non-silanized ZSM-5 prepared in the present work, show a FWHM value close to 6 ppm [28]. On the other hand, when a high Si_{pol}/Si_{gel} ratio is used, materials exhibiting less uniform aluminium environments are obtained, which is in agreement with the TEM micrographs wherein crystalline aggregates embedded in micrometer-size amorphous particles were observed. Indeed, the material synthesized from a Si_{pol}/Si_{gel} ratio = 0.12 evidences a FWHM value (11.5 ppm) next to amorphous silica-alumina (FWHM ~ 12 – 15 ppm) [42]. Considering the whole of these characterization data (XRD, FTIR, TEM), it seems that using $Si_{polymer}/Si_{gel}$ above

0.10 led inevitably to the partial/total formation of amorphous materials. Consequently, only the samples prepared with $Si_{polymer}/Si_{gel} \leq 0.10$ may be regarded properly as hierarchical ZSM-5. By comparison, the usage of larger size organosilanes (silylated polymer) allows incorporating lower amounts than with e.g. PHAPTMS without having observed the occurrence of amorphous materials.

In order to determine the whole pore size distribution of the samples prepared from different Si_{pol}/Si_{gel} ratios, Argon sorption experiments at 87 K were performed. Figure 4 displays the cumulative pore volume (CPV) and pore size distribution (PSD) derived applying the NLDFT method to the argon isotherm of every material. CPV`s and PSD`s of the samples prepared from different Si_{pol}/Si_{gel} ratios are compared with those of the sample synthesized omitting the addition of the silylated polymer. The first maximum detected around 5.2 Å in the PSD`s of the samples is associated with the adsorption in ZSM-5 zeolite micropores. The material prepared omitting the silanization step posses the highest argon adsorption in zeolite micropores, due to its higher crystal size compared with the samples prepared by silanization. Moreover, the amount of argon adsorbed in the ZSM-5 micropores diminishes as the Si_{pol}/Si_{gel} ratio employed in the silanization stage is enhanced, mainly when this ratio is higher than 0.05. Comparing this behavior with the observations derived from TEM, DRX and FTIR, it is possible to conclude that when a Si_{pol}/Si_{gel} ratio higher than 0.08 is used a certain proportion of amorphous phase is embodied in the synthesized material, increasing its proportion when the Si_{pol}/Si_{gel} ratio enhances. When a Si_{pol}/Si_{gel} ratio = 0.15 is used a completely amorphous material is obtained, with no significant amount of zeolite micropores being detected. Significant argon adsorption in pores between 20 and 60 Å, with a maximum centred close to 40 Å, is revealed in the CPV and PSD of this material. These pores are associated with voids generated by the organic moieties (TPA^+ and silylated polymer) occluded in the amorphous matrix before the calcination treatment. A similar mesopore size distribution is exhibited by the sample prepared from a Si_{pol}/Si_{gel} ratio = 0.12,

corroborating the presence of a high proportion of amorphous phase in this material. However, the mesopore size distribution of the material synthesized employing a Si_{pol}/Si_{gel} ratio = 0.10 shows a different shape, with a significant adsorption between 20 and 200 Å and a maximum around 50 Å. This fact must be related with the lessening in the proportion of amorphous phase in this sample with respect to the materials prepared employing a higher Si_{pol}/Si_{gel} ratio. As the proportion of amorphous phase diminishes (Si_{pol}/Si_{gel} ratio ≤ 0.08), the adsorption in pores with diameters higher than 200 Å becomes detectable. Although not being the main mesopore argon adsorption phenomenon, this behaviour can be attributed to intercrystal argon sorption or adsorption in the external surface of the aggregated nanoparticles and, in the series of materials prepared employing silylated polymer as organosilane, is only noticed if a well crystallized material is obtained. The materials synthesized employing Si_{pol}/Si_{gel} ratios of 0.05 and 0.03 show slightly different mesopore adsorption profiles. The material synthesized employing a Si_{pol}/Si_{gel} ratio = 0.03 exhibits a very important adsorption in pores with sizes ranging from 40 to 200 Å in diameter, with maxima detectable around 80-100 Å, while the sample prepared from a Si_{pol}/Si_{gel} ratio = 0.05 shows a lower adsorption between 20 and 200 Å with a not very clear maximum between 50-60 Å.

Table 1 summarizes the textural properties derived from argon adsorption-desorption measurements of the samples prepared employing a different Si_{pol}/Si_{gel} molar ratio. In line with the CPV and PSD graphics, as the Si_{pol}/Si_{gel} ratio employed in the silanization stage increases, surface area associated to zeolite micropores (S_{ZMP}) diminishes from 344 m^2/g (Si_{pol}/Si_{gel} ratio = 0.0) to 52 m^2/g (Si_{pol}/Si_{gel} ratio = 0.15), while the surface area related to the adsorption in non-zeolitic pores or secondary porosity (S_{SP}) increases from 74 m^2/g (Si_{pol}/Si_{gel} ratio = 0.0) to 467 m^2/g (Si_{pol}/Si_{gel} ratio = 0.15). Interestingly, by employing only a Si_{pol}/Si_{gel} ratio = 0.03 in the silanization stage it is possible to obtain a material with a secondary porosity three times higher than that of the non-silanized material (Si_{pol}/Si_{gel} ratio = 0.00). However, due to the fact that

surface area related to zeolite micropores diminishes as secondary porosity increases, a 30% reduction in zeolite micropore surface area for sample prepared from a Si_{pol}/Si_{gel} ratio of 0.03 is observed relative to the sample synthesized from a Si_{pol}/Si_{gel} ratio of 0.00. In addition, a remarkable result is that if Si_{pol}/Si_{gel} ratio applied in the silanization stage is lower than 0.10, synthesis yields achieved are close to 90% (wt% of solid product). However, for Si_{pol}/Si_{gel} ratio ≥ 0.10 synthesis yield diminishes from 72% (Si_{pol}/Si_{gel} ratio = 0.10) to 11% (Si_{pol}/Si_{gel} ratio = 0.15). It seems that, with the synthesis conditions tested in this work, a high proportion of silylated polymer in the synthesis gel hinders or inhibits the crystallization process precluding the aggregation of protozeolitic units in structures with a size enough to be recovered by centrifugation.

From a catalytic point of view, not only the accessibility of the active centres of the catalyst is important, but the number and strength of acid sites are also essential factors. Table 2 summarizes the acid properties of the samples prepared employing different Si_{pol}/Si_{gel} ratios. Si/Al atomic ratios, derived from ICP-AES, are close to 30 in all cases, with a slightly higher amount of Al being incorporated in most of the materials prepared by the protozeolitic silanization route. If every Al atom detected by ICP-AES had generated an active acid centre, the acidity values of the samples would be the ones reported in the Table 2 as Max. Theor. Acidity (Maximum Theoretical Acidity). Invariably, this value is higher than the experimental acidity measured by NH_3 TPD, and the percentage of the experimental acidity with respect to the percent maximum acidity (% Max. Acidity) diminishes as the proportion of silylated polymer added in the silanization stage increases. While a percentage near 100% is showed by the non-silanized sample, this value decreases to 45% when only a Si_{pol}/Si_{gel} ratio = 0.03 is employed in the silanization stage, and lower % Max. Acidity values around 30% are exhibited by the materials prepared from Si_{pol}/Si_{gel} ratios higher than 0.08.

As mentioned in the experimental section, NH_3 TPD analyses measure ammonia desorbed at temperatures above 180 ºC, consequently molecules adsorbed in centres of lower acid strength do not contribute to the experimental acidity. This fact would explain the lower values of acidity measured for the silanized samples. Additionally, the presence of mesopores over these samples would help the removal of ammonia at lower temperatures than in the reference ZSM-5, decreasing the reported acidity values as well. The acid strength of the catalysts, measured as the maximum temperature of ammonia desorption (T_{max}), diminishes as the Si_{pol}/Si_{gel} ratio increases. T_{max} declines from 370 ºC, in the non-silanized sample, to 310 ºC, in the sample synthesized from a Si_{pol}/Si_{gel} ratio = 0.03, while the materials prepared from Si_{pol}/Si_{gel} ratios higher than 0.08 exhibit a T_{max} reduction more than 100 ºC with respect to the non-silanized material. Due to the diminishing number and strength of acid sites detected, a poorer catalytic behaviour may be expected as the Si_{pol}/Si_{gel} ratio increases.

Samples silanized employing Si_{pol}/Si_{gel} molar ratios ranging from 0 to 0.12 were tested in the catalytic cracking of low density polyethylene (LDPE). The results can be found in Table 3, wherein the values of conversion, selectivity by groups and activity of the catalysts (turnover frequency, TOF) achieved in every reaction are shown. Really mild conditions were employed to conduct the reactions: a mass ratio plastic to catalyst (P/C) of 100 and a temperature of 340 ºC for 2 hours. As a consequence of these mild conditions a negligible conversion value is attained in the thermal cracking of LDPE (3.1%). However, using the non-silanized material (Si_{pol}/Si_{gel} ratio = 0.0) an appreciable conversion of 30% is achieved. At this point it is important to note that this non-silanized sample is a nanocrystalline ZSM-5, considered traditionally as a good catalyst in the feedstock recycling of polyolefins due to the good combination of acid and textural properties [41]. Very different conversion values are attained employing the silanized samples. The highest conversion (77%) is achieved with the catalyst prepared from a Si_{pol}/Si_{gel} ratio = 0.03. Although this catalyst posses a number of acid sites and an acid strength lower than the nanocrystalline

ZSM-5, its enhanced textural properties, with a secondary porosity three times higher than the later, improve access of the polyethylene macromolecules to the acid sites, and makes of this material a superior catalyst in the cracking of LDPE. The conversion diminishes to a value close to that of the non-silanized sample when the catalyst is prepared from a Si_{pol}/Si_{gel} ratio = 0.05. Although this material possesses a proportion of secondary porosity even higher than that of the ZSM-5 prepared from a Si_{pol}/Si_{gel} ratio = 0.03, the conversion achieved drops to a 27% because of the lower number and the weaker nature of its acid centres. A similar trend is observed in the samples prepared from a higher proportion of silylated polymer in the silanization stage, and despite the improved access to their catalytic sites much lower conversion values are attained due to their poorer acid properties. Values nearly 15% are achieved with samples employing a Si_{pol}/Si_{gel} molar ratio between 0.08 and 0.10, and fewer than 10% if a Si_{pol}/Si_{gel} ratio = 0.12 is used.

If the results of the catalytic cracking are evaluated in terms of activity (turnover frequency, TOF), a trend similar to that of the conversion is observed. In this reaction, two TOF parameters were used. Firstly, TOF (Si/Al -NH_3 TPD) was defined as grams of plastic converted to hydrocarbons (C_1-C_{16}) per grams of acid centres existing in the catalyst and per second. Likewise, TOF (Si/Al-ICP) was defined referred to the amount of Al atoms, assuming that each Al atom creates an acid centre. Both TOF values are reported in Table 3. In this case, the sample prepared from a Si_{pol}/Si_{gel} ratio = 0.03 shows the highest TOF (Si/Al – ICP) (0.491 s^{-1}), and, if a higher Si_{pol}/Si_{gel} molar ratio is applied, lower activities than that of the non-silanized sample are achieved, decreasing the TOF values as the Si_{pol}/Si_{gel} ratio increases. For the case of TOF (Si/Al-NH_3 TPD), it is considered that only the acid sites measured by NH_3 TPD are able to catalyze the cracking of LDPE. As expected, TOF (Si/Al-NH_3 TPD) values substantially differ from the TOF calculated from ICP. In all cases, enhanced TOF (Si/Al-NH_3 TPD) values are obtained in respect of TOF (Si/Al-ICP). Only a slight increase in activity is appreciated in the non-silanized sample,

because almost every Al atom generates a potential catalytically active acid site. However, all silanized materials exhibit a more than twice increase in TOF (Si/Al-NH_3 TPD) in respect of their corresponding TOF (Si/Al-ICP) values. Moreover, except for the material prepared from a Si_{pol}/Si_{gel} ratio = 0.12, the rest of silanized samples shows a higher TOF (Si/Al-NH_3 TPD) value than the non-silanized sample, indicating the improved accessibility of the active acid sites on these materials. In this case, due to the lower proportion and weaker strength of the active acid centres existing in the catalysts as Si_{pol}/Si_{gel} molar ratio increases, activity diminishes from 1.115 s^{-1} (Si_{pol}/Si_{gel} ratio = 0.03) to 0.185 s^{-1} (Si_{pol}/Si_{gel} ratio = 0.12).

Table 3 shows the selectivity data by groups obtained for LDPE cracking over the samples synthesized at different Si_{pol}/Si_{gel} molar ratio. Gaseous C_1-C_5 is the main fraction obtained in all the reactions, decreasing its proportion as the conversion attained in the reaction increases. Meanwhile, the percentage of the liquid C_6-C_{12} fraction increases with higher conversions. The main components obtained in the reactions are C_2-C_5 olefins, which decrease in selectivity as the catalyst activity increases (e.g. 55.7%, 59.8% and 69.2%, for catalyst prepared from Si_{pol}/Si_{gel} ratios of 0.03, 0.0 and 0.10, respectively). As the catalyst activity increases and the proportion of gaseous C_2-C_5 olefins decreases, the selectivity to olefins, naphtenics and aromatics hydrocarbons in the C_6-C_{12} fraction enhances. For example, the selectivity to the sum of olefins, naphtenes and aromatics in the gasoline range hydrocarbons diminishes from 32.9%, to 18.7% and finally to 10.3%, employing catalysts prepared from a Si_{pol}/Si_{gel} ratio of 0.03, 0.0, and 0.10, respectively. The later trends are according to an end-chain scission mechanism, characteristic of the HZSM-5, wherein gaseous C_3-C_5 olefins are the primary products. Subsequently, C_6-C_{12} aliphatic and aromatic hydrocarbons are formed by secondary reactions (oligomerization, cyclization and aromatization). On the other hand, liquid C_6-C_{12} fraction may also be obtained by direct catalytic cracking of the polymer. Besides this C_6 – C_{12} fraction,

valuable as gasoline, it is also noteworthy that around 25-50% of the main C_2-C_5 olefinic fraction is made up of propylene, 1-butene and isobutylene, which are useful petrochemical feedstocks.

In view of the excellent performance in the catalytic cracking of LDPE over the ZSM-5 sample prepared at a Si_{pol}/Si_{gel} ratio = 0.03, this catalyst was compared with a hierarchical ZSM-5 synthesized from silanized protozeolitic nanounits but using a smaller organosilane instead of silanized polypropylene diamine. In this case, the new sample was prepared adding phenyl-aminopropyl-trimethoxy-silane (PHAPTMS), and employing a $Si_{PHAPTMS}/Si_{gel}$ molar ratio of 0.05. In previous works, hierarchical ZSM-5 zeolites prepared from protozeolitic units silanization employing these conditions (view experimental section) have shown the highest activity in the catalytic cracking of polyolefins [36,37].

Figure 5 displays cumulative pore volume (CPV) and pore size distribution (PSD) derived applying the NLDFT method to the Ar sorption isotherms at 87K, of samples prepared employing PHAPTMS ($Si_{PHAPTMS}/Si_{gel}$ ratio = 0.05) and silylated polymer (Si_{pol}/Si_{gel} ratio = 0.03). For greater clarity, both hierarchical ZSM-5 zeolites were renamed as h-ZSM-5(PHAPTMS) and h-ZSM-5(SP), respectively. Nanocrystalline ZSM-5, the non-silanized sample synthesized omitting the presence of organosilanes is also depicted in Figure 5 for a comparative purpose only (n-ZSM-5). Hierarchical ZSM-5 zeolites synthesized employing different type of organosilanes shows a very different PSD profile. h-ZSM-5(PHAPTMS) displays a higher Ar sorption in zeolite micropores (maximum at 5.2 Å) than h-ZSM-5(SP), but the main difference is observed in the mesopore size distribution. While h-ZSM-5(SP) shows a remarkable adsorption in pores with sizes in the range 40-200 Å in diameter (maximum close to 100 Å), h-ZSM-5(PHAPTMS) exhibits principle adsorption in smaller pores with diameters ranging from 18 to 100 Å (maximum around 40 Å). Accordingly, the volume associated with adsorption in non-zeolitic micropores or secondary porosity (V_{SP}), is lower in h-ZSM-5(PHAPTMS) (0.307 cm^3/g) than in h-ZSM-5(SP) (0.534 cm^3/g). These values of textural properties derived from argon adsorption-desorption measurements are

summarized in Table 4, where on the other hand it is observed that h-ZSM-5(PHAPTMS) exhibits a higher value of BET (514 vs 449 m^2/g), zeolite micropore (279 vs 238 m^2/g) and secondary porosity (235 vs 211 m^2/g) surface area than h-ZSM-5(SP).

Table 5 shows the acid properties of the hierarchical ZSM-5 samples prepared employing both types of organosilanes. Despite existing a lower proportion of Al in h-ZSM-5(PHAPTMS) (higher Si/Al molar ratio), the highest acid strength and acidity is exhibited by this sample. Moreover, the percentage of the experimental acidity with regard to the maximum acidity is also higher in h-ZSM-5(PHAPTMS), showing a value close to 88%, denoting the improved acid properties of this sample in respect of h-ZSM-5(SP). On the other hand, the content of Brönsted acid sites was determined by means of titration techniques and the results are shown in Table 5. In this regard, the Brönsted protons (H^+) of the hierarchical zeolites were exchanged by Na^+ and titrated with a basic solution. By comparison, the reference ZSM-5 sample (0.0) exhibited a Brönsted acidity of 0.464 meq H^+ g^{-1}. The titration points out that h-ZSM-5 (SP) sample contains a considerably lower amount of Brönsted acid sites (0.250 meq H^+ g^{-1}) than h-ZSM-5 (PHAPTMS) (0.356 meq H^+ g^{-1}). Therefore, the usage of the silylated polymer seems to be clearly detrimental to obtain a high amount of strong acid sites and of Brönsted nature in the hierarchical ZSM-5, unlike it occurs with the PHAPTMS organosilane.

In order to evaluate the catalytic performance of both samples, exhibiting well different textural and acid properties each, cracking reactions of LDPE were carried out. The results in terms of conversion and activity are displayed in Figure 6. For comparison, conversion and activity attained employing the nanocrystalline ZSM-5 (non-silanized material) are also depicted. In spite of their different textural and catalytic properties, both hierarchical zeolites are excellent catalysts in the cracking of LDPE, and for the first time remarkable conversions have been attained at a temperature as low as 320 ºC. A 36% conversion value is obtained employing the h-ZSM-5(SP) sample at 320 ºC, a value higher than that attained with the non-silanized

nanocrystalline ZSM-5 at 340 ºC (30%). Comparing both hierarchical ZSM-5 zeolites, h-ZSM-5 (SP) exhibits slightly higher conversion values at both temperatures: 77% versus 71% at 340 ºC, and 36% versus 26% at 320 ºC, for h-ZSM-5(SP) and h-ZSM-5(PHAPTMS), respectively. In terms of the TOF values shown in Figure 6, at 340 ºC the h-ZSM-5(PHAPTMS) sample presents a quite higher TOF (Si/Al -ICP) value, calculated considering the whole aluminium content detected by ICP, than the h-ZSM-5(SP) sample. This fact implies that the h-ZSM-5(PHAPTMS) sample uses the aluminium in a higher extent and more effectively than the h-ZSM-5(SP) sample. However, if the TOF (Si/Al -NH_3 TPD) values, calculated considering only acid sites measured by NH_3 TPD are taken into account, the h-ZSM-5(SP) sample exhibits higher activity values than the h-ZSM-5(PHAPTMS) sample at both temperatures. The observed high performance of the h-ZSM-5(SP) despite its lower acid properties might be ascribed either to an unexpected activity in the cracking of polyolefins due to very weak acid sites or, more likely, to the improved accessibility of this sample due to the presence of large mesopores. In this regard, large mesopores may favour the diffusion of the bulky polymer and oligomer macromolecules leading toward high conversion values. Therefore, considering the whole of these data, it can be concluded that both hierarchical ZSM-5 samples display similar activities and for h-ZSM-5 (SP), the enhanced accessibility toward their acid sites seems to make up for the lower amount and strength of their acid sites.

With respect to the selectivity by groups achieved in the LDPE cracking reactions over both hierarchical ZSM-5 samples, gaseous C_1-C_5 is the main fraction obtained in the different reactions (close to 60%), although an important percentage of the gasoline range C_6-C_{12} fraction is also appreciated (around 40%), the fraction of heavier hydrocarbons (> C_{13}) being almost negligible. The product distribution per carbon atom number obtained in the catalytic cracking of LDPE, at 320 and 340 ºC, over both h-ZSM-5 samples is compared in Figure 7. Noteworthy, in the reactions carried out over the h-ZSM-5(SP), regardless of the temperature of reaction, the

product distribution hardly changes. However, as the temperature diminishes from 340 ºC to 320 ºC, a lower proportion of the medium C_6-C_{12} fraction is reached over the h-ZSM-5(PHAPTMS) catalyst. Apart from this, it seems clear that there is almost no difference in the product distribution per carbon atom number obtained over both hierarchical ZSM-5 samples at 340 ºC. However, in reactions carried out at 320 ºC, h-ZSM-5(SP) yields 6.2% less light C_4-C_5 hydrocarbons and 6.8% more C_6-C_9 products in comparison to h-ZSM-5(PHAPTMS). This means that according to the end-chain scission mechanism typical of the HZSM-5 zeolite explained earlier, at 320 ºC the h-ZSM-5(SP) sample exhibit a slightly higher activity than the h-ZSM-5(PHAPTMS), and light olefins generated as primary products are transformed in heavier hydrocarbons by secondary reactions in a slightly higher extent.

PIONA GC analyses were employed to determine the proportion of paraffins, olefins, isoparaffins, naphtenes and aromatics in the products generated from the conversion of LDPE at 320 ºC and 340 ºC over both h-ZSM-5 samples. Figures 8.A and B illustrate the composition by hydrocarbon types of the gas (C_1-C_5) and gasoline range (C_6-C_{12}) fractions, respectively. Figure 8.A shows that at both temperatures the gaseous products are mainly olefins produced by the end-chain scission mechanism. The composition of this fraction does not change significantly with the temperature in the conditions of reaction tested and the percentage of olefins is close to 86% when the h-ZSM-5(SP) is used, and slightly lower (84%) if h-ZSM-5(PHAPTMS) is used. Propylene, 1-butene, isobutene and trans-2-pentene are the main products obtained in the different reactions, being interesting feedstocks for the petrochemical industry. Moreover, the sum of the later compounds represents more than 50% by weight of the gaseous C_1-C_5 fraction when the reaction is performed over h-ZSM-5(SP), diminishing that percentage to 45% if the reaction is carried out over h-ZSM-5(PHAPTMS) sample. With regard to the gasoline range C_6-C_{12} fraction (figure 8.B), at both temperatures a slightly higher proportion of olefins, isoparaffins and naphtenes is reached with the h-ZSM-5(SP) in comparison to h-ZSM-5 (PHAPTMS). This fact

implies that primary end-chain scission and secondary oligomerization and cyclization reactions are promoted to a slightly higher extent over the h-ZSM-5(SP) sample. On the other hand, a quite higher proportion of n-paraffins and a slightly higher percentage of aromatics are attained over the h-ZSM-5(PHAPTMS) by comparison to h-ZSM-5(SP), the differences in regards to the aromatic fraction being more important at 340 ºC. As it is well known, the formation of aromatic compounds is promoted by strong acid sites; hence the last observations are in agreement with the higher strength of the acid sites on H-ZSM-5(PHAPTMS).

4. Conclusions

Bulky silylated polymers formed by reaction of a polypropylene oxide diamine (Jeffamine D-400) and an epoxisilane have proved to be suitable organosilanes for the synthesis of hierarchical ZSM-5 zeolites by crystallization of silanized protozeolitc nanounits. Well crystallized hierarchical zeolites and high synthesis yields (close to 90%) are achieved employing molar ratios of silica in the silylated polymer to silica in the synthesis gel (Si_{pol}/Si_{gel}) lower than 0.08. In terms of the catalytic performance in the cracking of low density polyethylene (LDPE), the optimum sample is that prepared from a Si_{pol}/Si_{gel} molar ratio of 0.03, with which despite the mild reaction conditions employed (T = 340 ºC, P/C = 100), a conversion close to 77% is reached. Moreover, a remarkable conversion of 36% is attained at a temperature as low as 320 ºC. By comparison with a hierarchical ZSM-5 attained employing a small organosilane (phenylaminopropyltrimetoxisilane, PHAPTMS), they differ in textural and acid properties. Both samples consist of aggregates of really small nanocrystals (10-20 nm), but the zeolite prepared from silylated polymers (SP) exhibits larger mesopores within the range 4 – 20 nm in a higher extent. However, the amount of their acid sites is lower and of less acid strength. Both samples show similar activity in the catalytic cracking of LDPE, suggesting that for h-ZSM-5 (SP), the enhanced accessibility due to

the larger mesopores seems to make up for the lower amount and strength of their acid sites. Accordingly, it is possible to enhance the mesoporosity by using bulkier organosilane (silylated polymer), although at the expense of losing acid properties.

Acknowledgements

The authors acknowledge financial support from “Ministerio de Ciencia e Innovación” in Spain (project TRACE: TRA2009/ 0111).

References

[1] D. P. Serrano; J. M. Escola and P. Pizarro. Chem. Soc. Rev. 42 (2013) 4004.

[2] J. Pérez-Ramírez, C. H. Christensen, K. Egeblad, C. H. Christensen and J. C. Groen. Chem. Soc. Rev. 37 (11) (2008) 2530.

[3] J. Cejka, G. Centi, J. Pérez-Pariente and W. J. Roth. Catal. Today. 179 (2012) 2.

[4] K. Egeblad, C. H. Christensen, M. Kustova and C. H. Christensen. Chem. Mater. 20(3) (2008) 946.

[5] C. H. Christensen, K. Johannson, E. Törnqvist, I. Schmidt, H. Topsoe and C. H. Christensen. Catal. Today. 128 (2007) 117.

[6] C. H. Christensen, K. Johannsen, I. Schmidt and C. H. Christensen. J. Am. Chem. Soc. 125 (2003) 13370.

[7] D. Mehlhorn, R. Valiullin, J. Karger, K. Cho and R. Ryoo. Microporous Mesoporous Mater. 164 (2012) 273.

[8] Z. Musilova, N. Zilkova, S. E. Park and J. Cejka. Top. Catal. 53(19-20) (2010) 1457.

[9] C. Fernández, I. Stan, J. P. Gilson, K. Thomas, A. Vicente, A. Bonilla and J. Pérez-Ramírez. Chem-Eur. J. 16(21) (2010) 6224.

[10] R. Srivastava, M. Choi and R. Ryoo. Chem. Commun. (2006) 4489.

[11] J. Kim, M. Choi and R. Ryoo. J. Catal. 269 (2010) 219.

[12] G. T. Kerr, J. Phys. Chem. 71 (1967) 4155.

[13] M. Ogura, S. Y. Shinomiya, J. Tateno, Y. Nara, M. Nomura, E. Kikuchi and M. Matsukata. Chem. Lett. (2000) 882.

[14] J. C. Groen, J. C. Jansen, J. A. Moulijn and J. Pérez-Ramírez. J. Phys. Chem. B. 108 (2004) 13062.

[15] J. Pérez-Ramírez, D. Verboekend, A. Bonilla and S. Abelló. Adv. Funct. Mater. 19 (2009) 3972.

[16] Y. Liu, W. Zhang and T. J. Pinnavaia. J. Am. Chem. Soc., Chem. Commun. 122 (2000) 8791.

[17] Y. Liu, W. Zhang and T. J. Pinnavaia. Angew. Chem. Int. Ed. 40(7) (2001) 1255.

[18] K. Na, C. Jo, J. Kim, K. Cho, J. Jeng, Y. Seo, R. J. Messinger, B. F. Chmelka and R. Ryoo. Science 333 (2011) 328.

[19] F. S. Xiao, L. Wang, C. Yin, K. Lin, Y. Di, J. Li, R. Xu, D. S. Su, R. Schlögl, T. Yokoi and T. Tatsumi. Angew. Chem. Int. Ed. 45 (2006) 3090.

[20] C. J. H. Jacobsen, C. Madsen, J. Houzvicka, I. Schmidt and A. Carlsson. J. Am. Chem. Soc. 122 (2000) 7116.

[21] I. Schmidt, A. Krogh, K. Wienberg, A. Carlsson, M. Brorson and C. J. H. Jacobsen. Chem. Commun. (2000) 2157.

[22] B. T. Holland, L. Abrams and A. Stein. J. Am. Chem. Soc. 121 (1999) 4308.

[23] Y. Tao, H. Kanoh and K. Kaneko. Langmuir 21 (2005) 504.

[24] M. Choi, H. S. Cho, R. Srivastava, C. Verkatesan, D. H. Choi and R. Ryoo. Nat. Mater. 5 (2006) 718.

[25] H. Wang and T. J. Pinnavaia. Angew. Chem. Int. Ed. 45 (2006) 7603.

[26] D. H. Park, S. S. Kim, H. Wang, T. J. Pinnavaia, M. C. Papapetrou, A. A: Lappas and K. S. Triantafyllidis. Angew. Chem. Int. Ed. 48 (2009) 7645.

[27] D. P. Serrano, J. Aguado, J. M. Escola, J. M. Rodriguez and A. Peral. Chem. Mater. 18 (2006) 2462.

[28] D. P. Serrano, J. Aguado, G. Morales, J. M. Rodriguez, A. Peral, M. Thommes, J. D. Epping and B. F. Chmelka. Chem. Mater. 21 (2009) 641.

[29] D. P. Serrano, J. Aguado, J. M. Rodríguez and A. Peral. Stud. Surf. Sci. Catal.170A (2007) 282.

[30] Z. Xue, J. Ma, W. Hao, X. Bai, Y. Kang, J. Liu and R. Li. J. Mater. Chem. 22(6) (2012) 2532.

[31] J. Aguado, D. P. Serrano and J. M. Rodríguez. Microporous Mesoporous Mater. 115 (2008) 504.

[32] J. Aguado, D. P. Serrano, J. M. Escola and A. Peral. J. Anal. Appl. Pyrolysis. 85 (2009) 352.

[33] D. P. Serrano, R. Sanz, P. Pizarro and I. Moreno. Chem. Commun. 171 (2009) 352.

[34] R. Srivastava, N. Iwasa, S. Fujita and M. Arai, Chem.-Eur. J. 14 (2008) 9507.

[35] Z. Xue, T. Zhang, J. Ma, H. Miao, W. Fan, Y. Zhang and R. Li. Microporous Mesoporous Mater. 151 (2012) 271.

[36] D. P. Serrano, J. Aguado, J. M. Escola, J. M. Rodriguez and A. Peral. J. Mater. Chem. 18 (2008) 4210.

[37] D. P. Serrano, J. Aguado, J. M. Escola, J. M. Rodriguez and A. Peral. J. Catal. 276 (2010) 152.

[38] D. P. Serrano, J. Aguado, J. M. Escola, A. Peral, G. Morales and E. Abella. Catal. Today 167 (2011) 86.

[39] T. Armaroli; L. J. Simon; M. Digne; T. Montanari; M. Bevilacqua; V. Valtchev; J. Patarin and G. Busca. Applied Catalysis A, 306 (2006) 78.

[40] G. Coudurier; C. Naccache and J. C. Vedrine. J. Chem. Soc., Chem. Commun. (1982) 1413.

[41] J. Aguado, D. P. Serrano, J. M. Escola and J. M. Rodríguez. Stud. Surf. Sci. Catal. 140 (2002) 77.

[42] E. Oldfield, J. Haase, K. D. Schmitt and S. E. Schramm. Zeolites. 14 (1994) 101

Table 1. Textural properties (Ar sorption measurements), optical density ratio (ODR, from FTIR spectra) and synthesis yield of the samples prepared from protozeolitic units silanization employing different Si_{pol}/Si_{gel} molar ratio.

Si_{pol}/Si_{gel} ratio	S_{BET} (m^2/g)	S_{ZMP} (m^2/g)	S_{SP} (m^2/g)	V_{TOT} (cm^3/g)	V_{ZMP} (cm^3/g)	V_{SP} (cm^3/g)	O.D.R. ($I_{550cm-1}/I_{450cm-1}$)	Yield (wt%)
0.0	420	344	74	0.403	0.198	0.205	0.864	93
0.03	449	238	211	0.671	0.137	0.534	0.893	81
0.05	446	222	244	0.498	0.128	0.370	0.830	96
0.08	498	191	307	0.525	0.110	0.415	0.819	91
0.10	532	142	390	0.565	0.082	0.483	0.747	72
0.12	536	95	441	0.372	0.055	0.317	0.689	29
0.15	519	52	467	0.346	0.030	0.316	0.654	11

Table 2. Acid properties of the samples synthesized employing different Si_{pol}/Si_{gel} molar ratio.

Si_{pol}/Si_{gel} ratio	ICP-AES	NH_3 TPD			
	Si/Al	T_{max} (ºC)	Acidity ($meqNH_3/g$)	Max. Theor. Acidity ($meqNH_3/g$)[1]	% Max. Acidity (%)[2]
0.0	36	370	0.433	0.452	95.8
0.03	24	310	0.300	0.670	44.8
0.05	24	283	0.252	0.670	37.6
0.08	30	270	0.209	0.539	38.8
0.10	25	260	0.180	0.644	30.0
0.12	26	260	0.191	0.620	30.8

[1] Maximum theoretical acidity assuming that every Al atom detected by ICP-AES generates an acid center.
[2] (Acidity (NH_3 TPD) / Max. Theor. Acidity) · 100

Table 3. Cracking of LDPE over the different ZSM-5 zeolite catalysts prepared from protozeolitic units silanization employing different Si_{pol}/Si_{gel} molar ratio (*T* = 340 ºC; g LDPE/g catalyst = 100; time = 2 h).

Si_{pol}/Si_{gel} ratio	**Conversion (%)**	**Selectivity by groups (wt%)**			**TOF (Si/Al-ICP) (s^{-1})**	**TOF (Si/Al-NH_3 TPD) (s^{-1})**
		$C_1 – C_5$	**$C_6 – C_{12}$**	**> C_{13}**		
No catal.	3.1	58.1	41.9	0.0	-	
0.0	30.0	72.3	27.5	0.2	0.293	0.305
0.03	77.0	57.1	42.2	0.7	0.491	1.115
0.05	27.3	71.7	28.3	0.0	0.179	0.486
0.08	16.1	75.4	24.6	0.0	0.144	0.378
0.10	14.1	83.4	16.6	0.0	0.104	0.381
0.12	7.4	86.2	13.8	0.0	0.056	0.185

Table 4. Textural properties (Ar sorption measurements) of ZSM-5 samples prepared employing different types of organosilanes: a silylated polymer, h-ZSM-5(SP) and phenyl-aminopropyl-trimetoxisilane, h-ZSM-5(PHAPTMS).

Sample	**S_{BET} (m^2/g)**	**S_{ZMP} (m^2/g)**	**S_{SP} (m^2/g)**	**V_{TOT} (cm^3/g)**	**V_{ZMP} (cm^3/g)**	**V_{SP} (cm^3/g)**
h-ZSM-5(SP)	449	238	211	0.671	0.137	0.534
h-ZSM-5(PHAPTMS)	514	279	235	0.468	0.161	0.307

Table 5. Acid properties of the hierarchical h-ZSM-5(SP) and h-ZSM-5(PHAPTMS) samples.

Sample	ICP-AES	NH_3 TPD				Brönsted acidity (meq.H^+/g)[3]
	Si/Al	T_{max} (ºC)	Acidity (meqNH_3/g)	Max. Theor. Acidity (meqNH_3/g)[1]	% Max. Acidity (%)[2]	
h-ZSM-5(SP)	24	310	0.300	0.670	44.8	0.250
h-ZSM-5(PHAPTMS)	32	360	0.444	0.507	87.6	0.356

[1] Maximum theoretical acidity assuming that every Al atom detected by ICP-AES generates an acid center.
[2] (Acidity (NH_3 TPD) / Max. Theor. Acidity) · 100
[3] Determined by titration with a basic solution

Figure captions:

Figure 1: A, XRD patterns, and B, FTIR spectra of the calcined samples synthesized employing different Si_{pol}/Si_{gel} molar ratios.

Figure 2: TEM micrographs of the samples synthesized employing different Si_{pol}/Si_{gel} molar ratios: a) 0.0, b) 0.03, c) 0.03, d) 0.05, e) 0.08, f) 0.1 g) 0.1. h) 0.1 i) 0.12.

Figure 3: ^{27}Al MAS NMR of selected calcined samples synthesized employing different Si_{pol}/Si_{gel} molar ratios.

Figure 4: Pore-size distributions and cumulative pore volumes of the calcined samples obtained from NLDFT calculations applied to the adsorption branch of the Ar adsorption-desorption isotherms at 87 K.

Figure 5: Comparison of pore-size distributions and cumulative pore volume of hierarchical ZSM-5 samples: h-ZSM-5(SP) and h-ZSM-5(PHAPTMS).

Figure 6: Conversion and activity in the cracking of LDPE over both hierarchical ZSM-5 samples and n-ZSM-5 (g LDPE/g catalyst = 100; time = 2 h).

Figure 7: Selectivity by carbon atom number obtained in the cracking of LDPE over hierarchical ZSM-5 samples (g LDPE/g catalyst = 100; time = 2 h).

Figure 8: Composition of: (A) C_1-C_5, (B) C_6-C_{12} fractions, respectively, obtained in the cracking of LDPE over hierarchical ZSM-5 samples (g LDPE/g catalyst = 100; time = 2 h).

Figures:

Figure 1

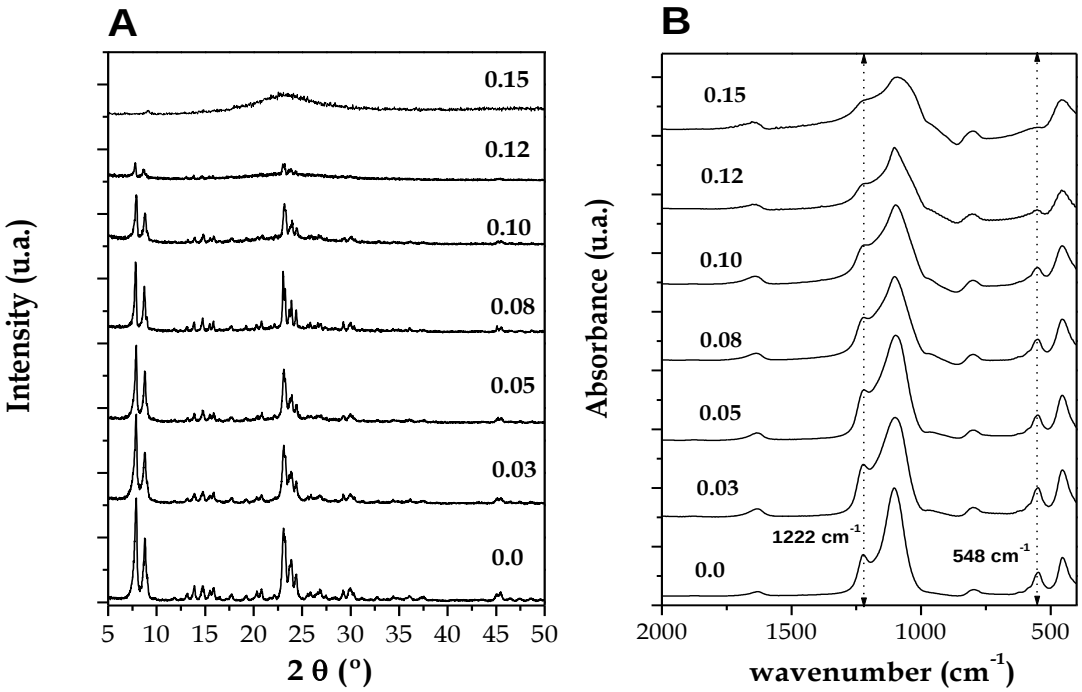

Figure 2

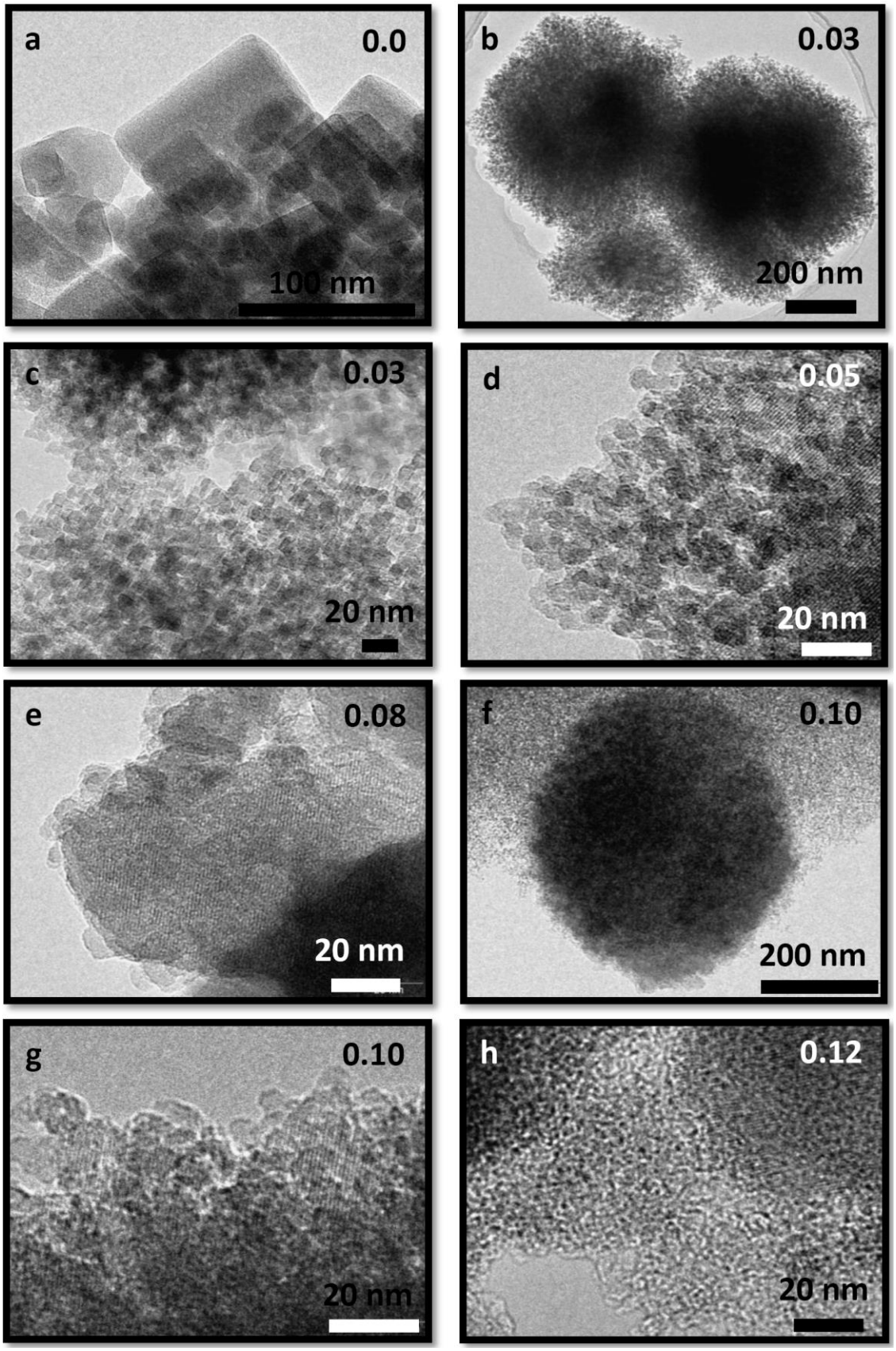
a
0.0
100 nm
b
0.03
200 nm
c
0.03
20 nm
d
0.05
20 nm
e
0.08
20 nm
f
0.10
200 nm
g
0.10
20 nm
h
0.12
20 nm

Figure 3

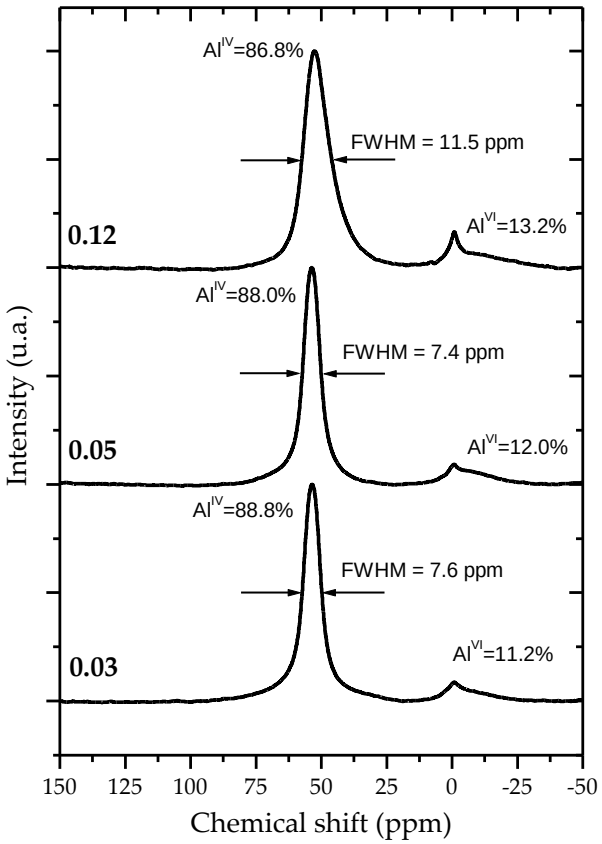
Al^IV=86.8%
FWHM = 11.5 ppm
Al^VI=13.2%
0.12
Al^IV=88.0%
FWHM = 7.4 ppm
Al^VI=12.0%
0.05
Al^IV=88.8%
FWHM = 7.6 ppm
Al^VI=11.2%
0.03
Intensity (u.a.)
150 125 100 75 50 25 0 -25 -50
Chemical shift (ppm)

Figure 4

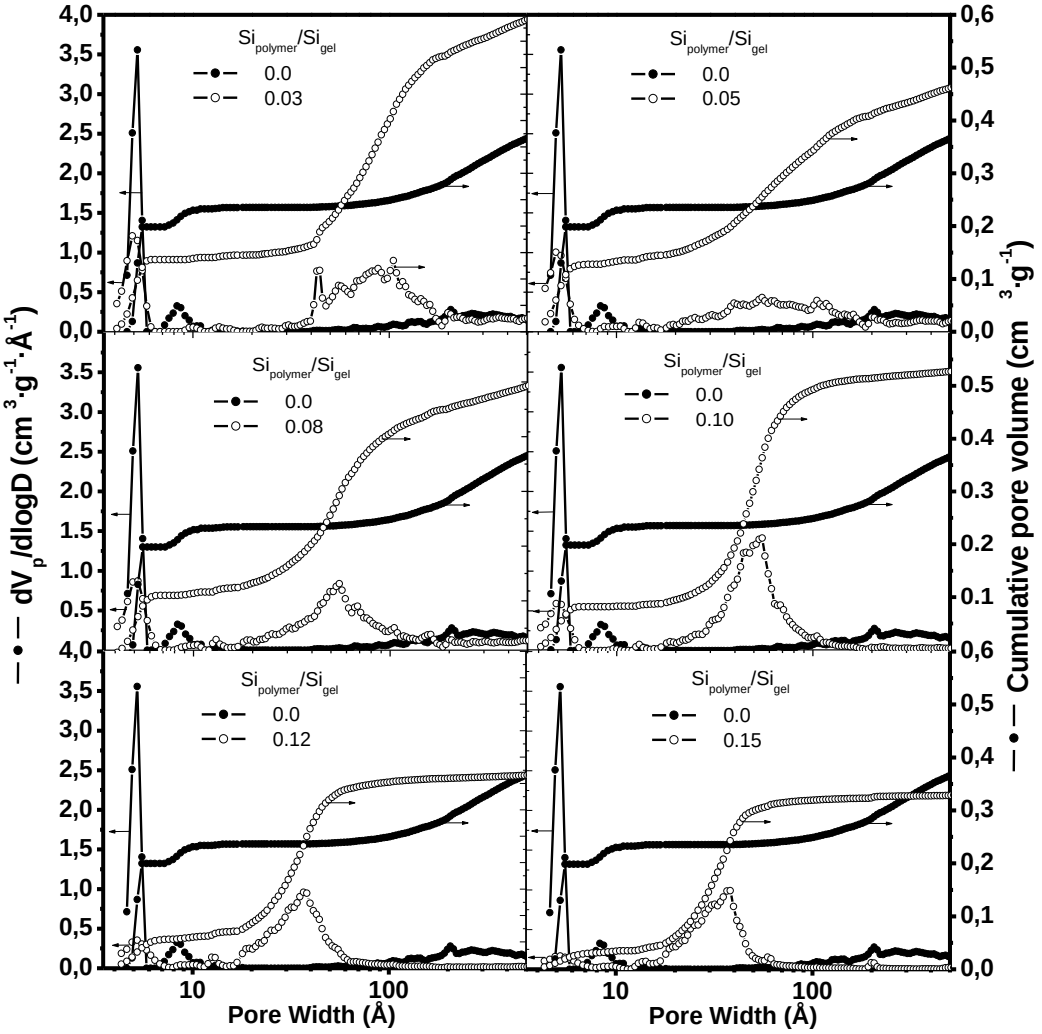
Si_polymer/Si_gel
0.0
0.03
0.05
0.08
0.10
0.12
0.15
— ● — dV_p/dlogD (cm ³·g⁻¹·Å⁻¹)
— ● — Cumulative pore volume (cm ³·g⁻¹)
Pore Width (Å)
10
100

Figure 5

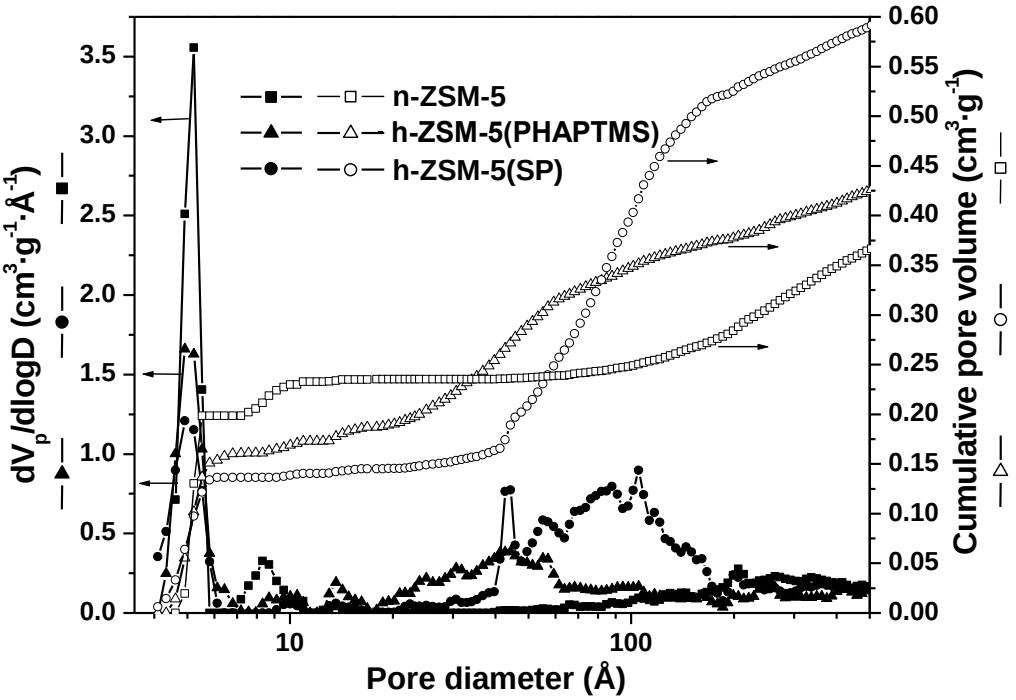
n-ZSM-5
h-ZSM-5(PHAPTMS)
h-ZSM-5(SP)
dV_p/dlogD (cm^3·g^-1·Å^-1)
Cumulative pore volume (cm^3·g^-1)
Pore diameter (Å)
0.0
0.5
1.0
1.5
2.0
2.5
3.0
3.5
0.00
0.05
0.10
0.15
0.20
0.25
0.30
0.35
0.40
0.45
0.50
0.55
0.60
10
100

Figure 6

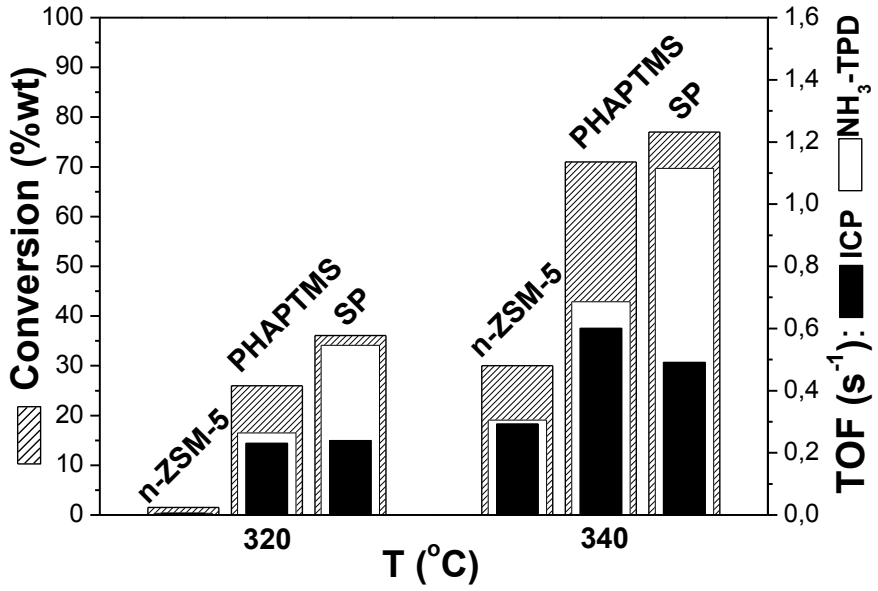
Conversion (%wt)
TOF (s^{-1}): ICP NH_3-TPD
n-ZSM-5
PHAPTMS
SP
n-ZSM-5
PHAPTMS
SP
320
340
T (°C)

Figure 7

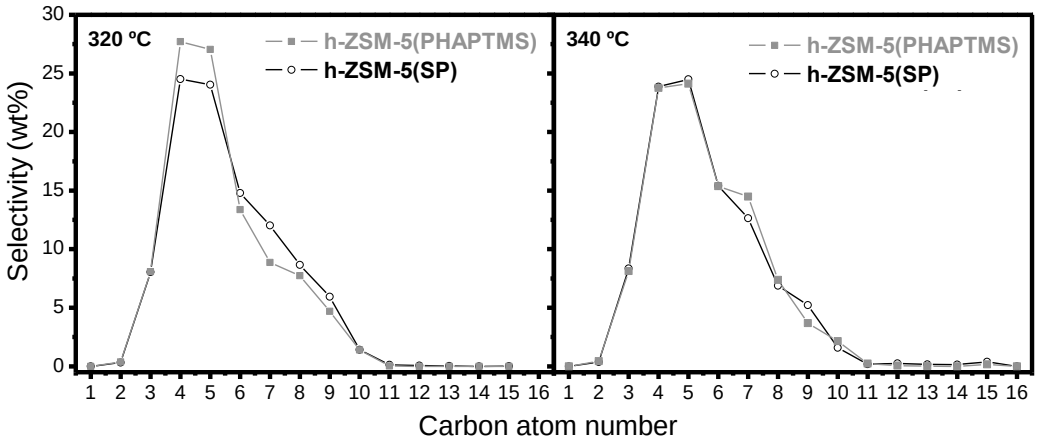
320 ºC
340 ºC
h-ZSM-5(PHAPTMS)
h-ZSM-5(SP)
Selectivity (wt%)
Carbon atom number
0
5
10
15
20
25
30
1 2 3 4 5 6 7 8 9 10 11 12 13 14 15 16

Figure 8

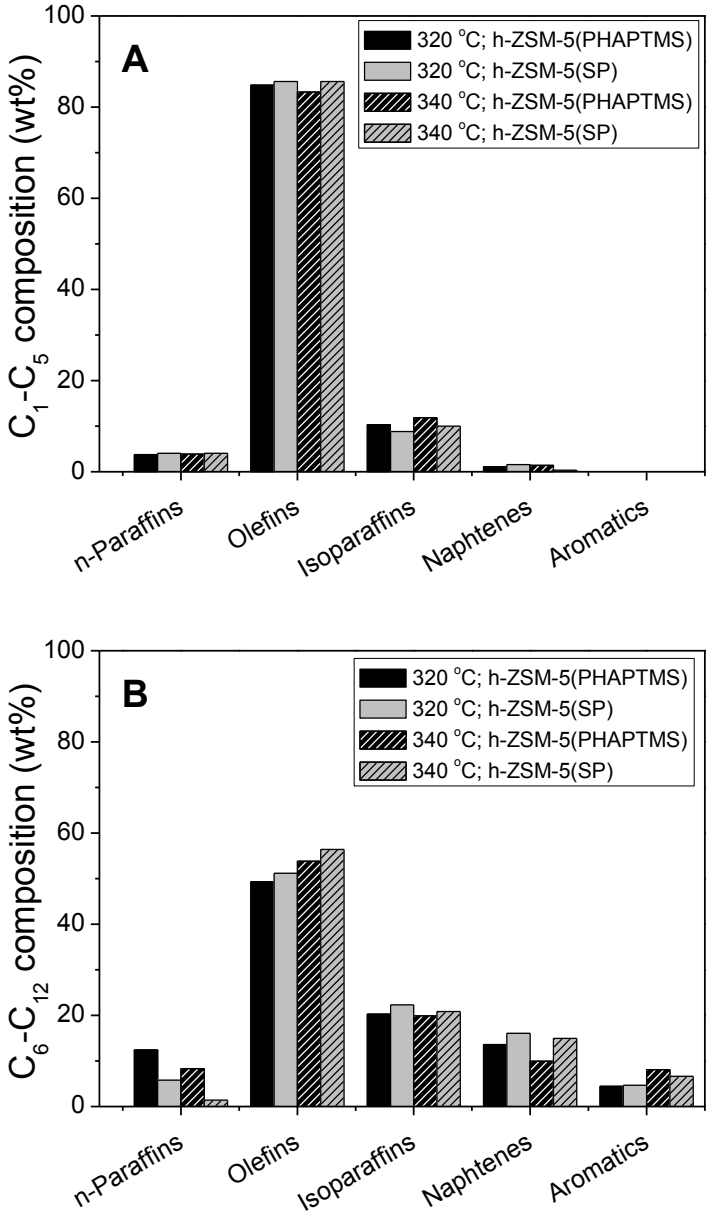
A
320 °C; h-ZSM-5(PHAPTMS)
320 °C; h-ZSM-5(SP)
340 °C; h-ZSM-5(PHAPTMS)
340 °C; h-ZSM-5(SP)
C1-C5 composition (wt%)
0
20
40
60
80
100
n-Paraffins
Olefins
Isoparaffins
Naphtenes
Aromatics
B
320 °C; h-ZSM-5(PHAPTMS)
320 °C; h-ZSM-5(SP)
340 °C; h-ZSM-5(PHAPTMS)
340 °C; h-ZSM-5(SP)
C6-C12 composition (wt%)
0
20
40
60
80
100
n-Paraffins
Olefins
Isoparaffins
Naphtenes
Aromatics